

Studies of the electronic phase transition in $\text{Lu}_5\text{Ir}_4\text{Si}_{10}$ and $\text{Lu}_5\text{Rh}_4\text{Si}_{10}$ by ^{175}Lu -NMR

Po-Jen Chu and B. C. Gerstein

Department of Chemistry and Energy and Mineral Resources Research Institute, Iowa State University, Ames, Iowa 50010

H. D. Yang and R. N. Shelton

Ames Laboratory—U.S. Department of Energy and Department of Physics, Iowa State University, Ames, Iowa 50010

(Received 16 July 1987)

Pulsed nuclear magnetic resonance of ^{175}Lu ($I = \frac{7}{2}$) was used to study the electronic phase transition of samples $\text{Lu}_5\text{Ir}_4\text{Si}_{10}$ and $\text{Lu}_5\text{Rh}_4\text{Si}_{10}$ under atmospheric pressure from 49 to 310 K. A calculation of the powder line shape in the quadrupole regime for $I = \frac{7}{2}$ shows that the critical frequencies, particularly that of the singularity, are sensitive to the change of the electric-field-gradient (EFG) asymmetry and the Larmor frequency. From the singularity near $\nu = \nu_0$, the EFG asymmetry of the lutetium nucleus is estimated to be $\eta \approx 0.4$. The temperature coefficient of the lutetium EFG asymmetry as estimated from the temperature-dependent shift is close to $3 \times 10^{-5} \text{ K}^{-1}$. This small variation of the EFG asymmetry suggests that the crystal structure remains unchanged in the temperature range studied. The possible formation of charge-density-wave states at 83 and 145 K for the two compounds, respectively, is indicated by anomalous variations of the temperature-dependent Knight shift. A loss of the electronic density of states at the Fermi level, as inferred from the jump discontinuity of the Knight shift, is consistent with previous measurements of resistivity and the magnetic susceptibility on these samples. From the correlation of the Knight shift with the magnetic susceptibility, the hyperfine field is determined to be 0.5 and 0.7 MOe, a value consistent with the previous measurements of rare-earth metals. The NMR of ^{45}Sc ($I = \frac{7}{2}$) in $\text{Sc}_5\text{Ir}_4\text{Si}_{10}$, isostructural with the above two compounds, was used as a baseline measurement to illustrate the anomalous behavior observed for ^{175}Lu in $\text{Lu}_5M_4\text{Si}_{10}$ ($M = \text{Ir, Rh}$).

INTRODUCTION

$\text{Lu}_5\text{Ir}_4\text{Si}_{10}$ shows a phase transition at 79 K as indicated by the electrical resistivity and static magnetic susceptibility at ambient pressure.¹ The transition temperature for the electrical resistivity decreases under applied pressure, and is completely suppressed at the critical pressure $P_c = 21$ kbar. In addition, the removal of this phase transition results in a large, discontinuous enhancement of the superconducting temperature from 3.8 to 9.1 K. Other experiments, for instance, bulk modulus and low-temperature powder x-ray diffraction indicate no detectable deviation from the primitive tetragonal symmetry.² All results suggest that the transition is electronically driven, e.g., by the formation of a charge-density-wave (CDW) state, rather than being associated with a change in the lattice symmetry.

It has been estimated from the magnetic susceptibility and the heat capacity that a 36% loss of the density of electronic states at the Fermi level occurs at the transition temperature for $\text{Lu}_5\text{Ir}_4\text{Si}_{10}$.¹ This behavior is consistent with the notion that there exists a Peierls-type phase transition which produces a periodic lattice distortion (PLD) that is accompanied by the formation of an incommensurate-charge-density-wave state (ICDW) associated with the opening of the energy gap over portions of the Fermi surface and the loss of the density of electronic state.³

$\text{Lu}_5\text{Rh}_4\text{Si}_{10}$, another ternary rare-earth transition-metal silicide, possesses the same $\text{Sc}_5\text{Co}_4\text{Si}_{10}$ -type struc-

ture as $\text{Lu}_5\text{Ir}_4\text{Si}_{10}$. The physical properties and the anomalies in resistivity and susceptibility are similar to those observed in $\text{Lu}_5\text{Ir}_4\text{Si}_{10}$ except that the electronic transition occurs at 145 K.² The anomalies in resistivity and susceptibility are, however, not as pronounced in the Rh as in the Ir compound.

Since the NMR frequency of quadrupolar nuclei in metals is a sensitive function of the free-electron density and the electric-field gradient at the nucleus, NMR of such nuclei probes matter at a local and microscopic level, allowing one to infer information about the static and the dynamic behavior of solids. The purpose of this study is to use NMR of a strong quadrupole nucleus as a means of monitoring the electronic phase transition in $\text{Lu}_5M_4\text{Si}_{10}$ ($M = \text{Ir, Rh}$).

Although studies of quadrupole nuclei by NMR have received increasing attention recently, most of the work has been limited to systems with relatively weak quadrupole moments, particularly to noninteger quadrupole nuclei where the half-half central transition is of order of a few to a few tens kHz. In the present study of the electronic phase transitions by NMR of a quadrupolar nucleus, the nucleus in question, ^{175}Lu ($I = \frac{7}{2}$), has a strong quadrupole moment of 4.5 to 6.8 barns ($\equiv 10^{-24} \text{ cm}^2$) from different sources.^{4,5} For such species, the quadrupolar coupling constant, e^2qQ , can be as high as few GHz.^{5,6} This value is much larger than the Larmor frequency of the current available magnetic fields ($\approx 10^2 \text{ MHz}$). Therefore in this regime, previous results using the quadrupolar Hamiltonian as a perturbation on the Zeeman interaction cannot be applied. To relate the

observed spectra to quadrupolar and shielding interactions, it is necessary to solve the problem in which all Hamiltonians including the Zeeman are exactly taken into account.

Most NMR studies on metal-semiconductor or other electronic phase transitions have been performed on oriented single crystals or pseudomonocrystals (a group of crystals aligned along a fixed axis), or by zero-field nuclear quadrupole resonance (NQR) of powders.⁷⁻¹¹ Only a relatively small number of studies of the CDW state on powdered samples have been reported. Devreus¹² has studied the ICDW phase transition of NbSe₃ by ⁹³Nb NMR powdered spectrum. Natio *et al.*¹³ have used ¹⁸¹Ta NMR to study the charge-density-wave state of 1*M*-TaSe₂ and 1*I*-TaS₂ in powder. These measurements however, only served to provide results complementary to single-crystal studies. A typical problem is that a single crystal of sufficient size for the required sensitivity in NMR measurements is not always available. Therefore to investigate the NMR spectra of polycrystalline samples, as affected by an electronic transition such as formation of the ICDW state, knowledge of the polycrystalline spectra in the quadrupole regime are desirable.

The skin-depth effect poses one further problem to NMR measurements in metals. This factor reduces the effective sample volume of bulk samples and, therefore, the sensitivity of the measurement unless the particle size is of the order of, or smaller than, the skin depth. This depth is typically less than 1 μm in rare-earth metals. Powder samples with particles of this size may not be representative of the physical phenomena probed by NMR. Another consequence of the skin-depth effect is the exponential decrease of the rf field through the sample causing different degrees of rf excitation of the nucleus studied. Both effects results in an admixture of absorption and dispersion modes in both cw and pulsed NMR experiments.

One final consideration in applying pulsed NMR to metals is that limited rf power homogeneously excites only the transitions within $1/(2t_p)$ of the carrier. The flip angle $\theta = t_p \gamma B_1$ decreases rapidly beyond this frequency range. When the spectrum is much wider than the rf strength, the observed spectrum will be severely distorted and attenuated.^{4,6} As will be derived later in the calculation, NMR resonance frequencies of strong quadrupole polycrystalline samples may range from $0.3\nu_0$ to $7.0\nu_0$ for spin $I = \frac{7}{2}$ nucleus. It is impossible to homogeneously excite this spectral width by experimentally available B_1 fields.

These factors make the observation of a complete polycrystalline powder spectrum in the strong quadrupole regime practically impossible. Segel and Barnes have previously reported the feasibility and value of observing NMR at the singularity frequencies for polycrystalline samples in the quadrupole regime.¹⁴ In their studies of a spin $\frac{3}{2}$ species, this frequency was equal to $2\nu_0$ for an axially symmetric electron-field-gradient (EFG) tensor. Applications of this idea have been extended to study the asymmetry and quadrupole constants of strong quadrupolar nuclei by variable magnetic field measurements.^{15,16} The principle of monitoring the

critical frequencies in NMR spectra of polycrystalline samples is equally applicable to strong quadrupolar nuclei with spin other than $I = \frac{3}{2}$ and to nonaxial symmetric EFG tensors, providing the critical frequencies can be described in terms of the Zeeman and quadrupolar interactions. Hence in the first part of the study, the position of these critical frequencies for various spins as a function of the quadrupole and Zeeman interaction parameter, such as the EFG asymmetry and the Larmor frequency, are determined.

These results will be used later to probe the anomalous behavior in resistivity and magnetic susceptibility of Lu₅Ir₄Si₁₀ and Lu₅Rh₄Si₁₀ via the temperature dependence of the frequency shift.

The nucleus ¹⁷⁵Lu was chosen as the NMR active nucleus for study because it has a strong hyperfine magnetic field interaction H_d compared to the other nuclei in the sample. This makes the spectrum quite sensitive to changes in electronic environment. The much larger gyromagnetic ratio as compared with Ir or Rh yields higher sensitivity for the transient NMR experiment.

As a baseline comparison with the NMR of ¹⁷⁵Lu in powdered Lu₅Ir₄Si₁₀ and Lu₅Rh₄Si₁₀, the NMR of the ⁴⁵Sc ($I = \frac{7}{2}$) NMR in Sc₅Ir₄Si₁₀ was determined as a function of temperature from 70 to 300 K. This compound, which possesses the same crystal structure as Lu₅Ir₄Si₁₀ with the lutetium ion being replaced by Sc, exhibits no electronic transition as inferred from the resistivity and susceptibility measurement in the temperature range below 300 K.

EXPERIMENTAL

Samples of Lu₅Ir₄Si₁₀, Lu₅Rh₄Si₁₀, and Sc₅Ir₄Si₁₀ were prepared by arc melting stoichiometric mixtures of high-purity elements in a Zr-gettered argon atmosphere. The resulting ingots were turned over and remelted at least 5 times to promote homogeneity. The samples were then sealed in quartz ampoules with about 160 Torr of argon and annealed at 1250°C for one day, followed by an anneal for seven days at 1050°C. Powder x-ray diffraction measurements confirm that the material crystallized in the Sc₅Co₄Si₁₀-type structure, as shown in Fig. 1. The lattice parameters are detailed elsewhere.¹⁷

Bulk samples of Lu₅Rh₄Si₁₀, Lu₅Ir₄Si₁₀, and Sc₅Ir₄Si₁₀ were shaped in approximate dimensions of 4 mm diameter and 7 mm long and sealed under ambient pressure in the 5 mm NMR tubes.

The NMR experiments were performed on a home-built NMR spectrometer previously described¹⁸ which utilizes a 5.2 T Nicolet superconducting magnet of 51 mm bore. This field gives a Larmor frequency of $\nu_0 = 25$ MHz for ¹⁷⁵Lu ($I = \frac{7}{2}$) and $\nu_0 = 53.5$ MHz for ⁴⁵Sc ($I = \frac{7}{2}$).

The variable temperature NMR probes were home built. The precision of the temperature control was approximately half a degree. During variable temperature experiments the power of the transmitter was maximized and maintained at 1 kW, which produced a 3 μs $\pi/2$ pulse at 28 MHz for ¹³³Cs in saturated CsCl aqueous solution. The probe was then returned to 25 MHz for

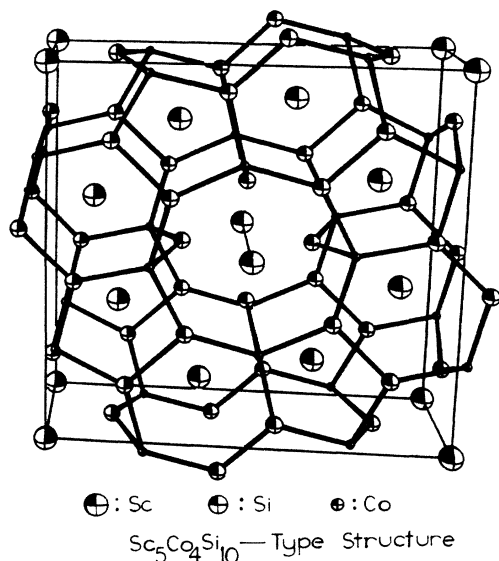


FIG. 1. Projection of the $\text{Sc}_5\text{Co}_4\text{Si}_{10}$ -type structure along [001]. The three ternary transition-metal silicides studied possess the same $\text{Sc}_5\text{Co}_4\text{Si}_{10}$ -type structure. The large circle corresponds to the rare-earth element Lu or Sc, the larger dots represent the transition metals Ir, Rh, or Co, while silicon occupies the vertices indicated by the small dots.

measurements on ^{175}Lu .

Lutetium exhibits a quadrupole coupling constant in the range of few GHz. In the quadrupole regime, the only signal that can be observed clearly in NMR of a powder samples for the transition between the two lowest lying levels, is the singularity corresponding to the orientation of the EFG x axis being parallel to the Zeeman z axis (*vide infra*). In order to optimize the observation of this singularity for the $(\frac{1}{2}, -\frac{1}{2})$ transition, the pulse tipping angle was reduced to approximately 22.5° according to the scaling relation, $(I + \frac{1}{2})$.^{6,19} This angle corresponds to a pulse width of $0.5 \mu\text{s}$ in 1 kW transmitter power and a spectral width of 1 MHz at the 3 db points. Experimentally, this flip angle yielded the maximum spectra intensity, and produced a more homogeneous excitation over a broader spectral range compared to a 90° flip angle.

The singularity in the $(\frac{1}{2}, -\frac{1}{2})$ transition of ^{175}Lu observed in the quadrupole regime was shifted approximately 3 kHz/deg in the variable temperature studies. To minimize distortion and attenuation caused by the large resonance offset, the probe was retuned for each different temperature and the carrier frequency was shifted such that the frequency of the rf field was always close to the singularity frequency for each temperature. The transient signals were quadrature detected and transformed.

The NMR of the intermediate strength quadrupolar nucleus ^{45}Sc in $\text{Sc}_5\text{Ir}_4\text{Si}_{10}$ was measured in the same magnetic field after retuning the variable temperature probe to 53.5 MHz. Spectrometer tuning of these experiments was done on ^{13}C of enriched acetic acid which resonates above 2 MHz above the resonance frequency of ^{45}Sc .

The sample chamber temperature was controlled by a flow of liquid helium or liquid nitrogen. A Constantan

versus Alumel thermocouple monitored the sample temperature to an accuracy of ± 1.0 K. The lowest stable attainable temperature was 49 K. Beyond this temperature, the rf coil began to arc discharge in the helium gas.

An estimation of T_1 was obtained through progressive saturation of the transient signal after a string of $\pi/2$ pulses separated by variable spacing τ . These values of T_1 ranged from 1 ms at 77 K to 20 ms at 300 K for lutetium. Hence a recycle time of 160 ms was used at all temperatures for studies of both $\text{Lu}_5\text{Ir}_4\text{Si}_{10}$ and $\text{Lu}_5\text{Rh}_4\text{Si}_{10}$.

The receiver dead time and giant pulse breakthrough was reduced to $5.5 \mu\text{s}$, after series L - C circuits were inserted²⁰ between each stage of the video amplifier. A linear phase correction was performed for all spectra due to the truncation of the initial time decay. This operation, however, does not correct the mixing of the absorption and the dispersion modes associated with the skin-depth effect.

For all experimental spectra shown in the figures, upfield is drawn towards the right in the direction of decreasing frequency.

CALCULATION

The character and features of the line shape of NMR spectra of polycrystalline samples in the quadrupole regime are now discussed. In the previous studies of spin $I = \frac{3}{2}$ nuclei, an analytical expression was used for the transition frequency which drastically reduced the complexity of the calculation of the powder line shape.¹⁴⁻¹⁶ This expression is only valid for the first-order perturbation treatment of spin $\frac{3}{2}$ case and axially symmetry case for $I = \frac{5}{2}$. For a more general combination of Zeeman and quadrupole interaction parameters, and particularly for nonspin $\frac{3}{2}$ nuclei, an exact calculation must be performed. The calculation of the powder line shape involving the determination of the transition frequencies and the transition probabilities for the total Hamiltonian composed of both Zeeman and quadrupole interactions to first-order approximation has previously been performed.²¹ Details of the current exact calculation will be reported elsewhere.²² For the present purpose, the procedures of the calculation are briefly described and the calculated spectra are discussed qualitatively.

The powder spectra in the quadrupole regime is calculated after averaging over all the random orientations characterized by angles (θ, ϕ) . The transition between the two lowest states, $|\frac{1}{2}\rangle$ and $|\frac{1}{2}\rangle$ are shown in Figs. 2(a), 2(b), and 2(c), respectively, for spin $I = \frac{3}{2}$, $I = \frac{5}{2}$, and $I = \frac{7}{2}$. The transient decay $\langle I_y(t) \rangle$ is calculated first, followed by the powder average. Finally, Fourier transformation $\langle I_y(t) \rangle$ yields the powder spectrum. The time increment of the decay is chosen to be the inverse of the total frequency interval, i.e., $10\nu_0$, $7.5\nu_0$, and $4\nu_0$, respectively, for the three spins. The angle θ ranges from 0 to $\pi/2$, and ϕ ranges from 0 to π , with a 2° mesh for both angles in the powder average. Before Fourier transformation, the transient signal $\langle I_y(t) \rangle$ is multiplied by a Lorentzian decay function to account for residual homogeneous broadening. The

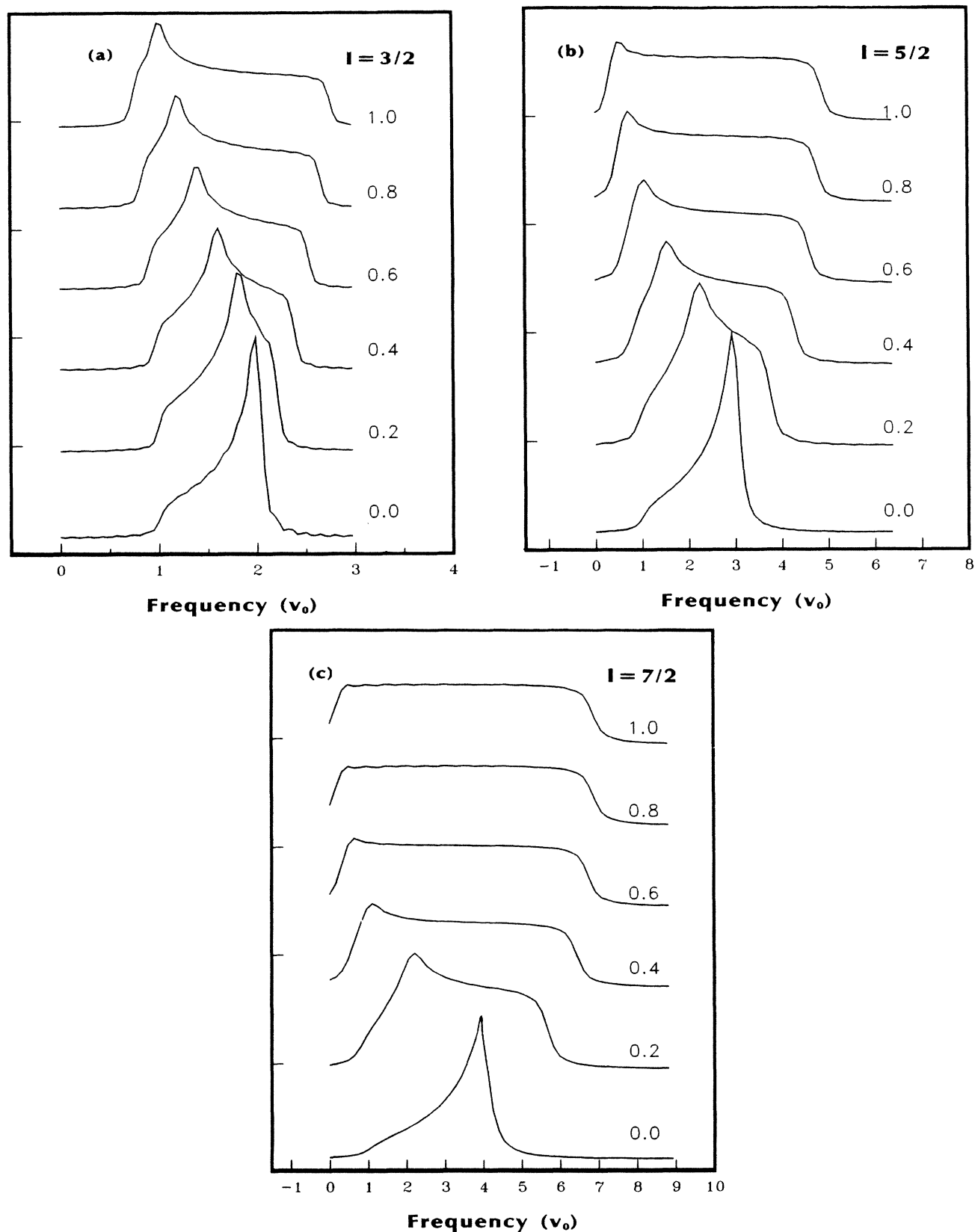


FIG. 2. Exact calculation of the polycrystalline spectra in the quadrupole regime for spin: (a) $I = \frac{3}{2}$, (b) $I = \frac{5}{2}$, and (c) $I = \frac{7}{2}$. The calculation uses $\nu_q = 40\nu_0$. The spectra are shown for asymmetry parameter $\sigma \leq \eta \leq 1$ in steps of 0.2. All frequencies are illustrated in units of the Larmor frequency, ν_0 . The critical frequencies correspond to the following spectral features and EFG orientations: (1) a singularity, where magnetic field is parallel to the x axis of the EFG tensor, (2) a high-frequency step where \mathbf{B}_0 is parallel to EFG y axis, and (3) a low-frequency shoulder where the field is parallel to the EFG z axis.

half-widths of the Lorentzian broadening function are: $I = \frac{3}{2}$, $\Delta = 1.2\nu_0$, $I = \frac{5}{2}$, $\Delta = 0.7\nu_0$, and $I = \frac{7}{2}$, $\Delta = 1.2\nu_0$. Application of the broadening function smooths the calculated spectra and allows the use of a coarser mesh and drastically shortens the calculation time. In fact, using a finer mesh does not improve the calculation with this broadening half-width.

The powder spectra are seen to be sharply dependent upon the asymmetry of the EFG tensor but less so upon the quadrupole coupling constants as expected. Three critical frequencies corresponding to a singularity, a step, and a shoulder can be found in all the calculations. The singularity corresponds to the orientation $\theta = 90^\circ$, $\phi = 0$, i.e., the principal EFG x axis being parallel to the magnetic field, which is the Zeeman z axis. For the axially symmetric case ($\eta = 0$), this frequency is at $2\nu_0$ for $I = \frac{3}{2}$, $3\nu_0$ for $I = \frac{5}{2}$, and $4\nu_0$ for $I = \frac{7}{2}$. The high-frequency step corresponds to the orientation where the EFG y axis is coincident with the magnetic field. This frequency extends as far as $7\nu_0$ for spin $I = \frac{7}{2}$ for the nonaxially symmetric case ($\eta = 1.0$). The lower-frequency shoulder is associated with the magnetic field being coincident with the EFG z axis. This frequency never extends beyond ν_0 . The lowest frequency of this shoulder occurs for $\eta = 1.0$, which is $0.7\nu_0$ for $I = \frac{3}{2}$, $0.4\nu_0$ for $I = \frac{5}{2}$, and $0.3\nu_0$ for $I = \frac{7}{2}$.

Results of the exact calculation reported here [Fig. 2(a)] are identical to that given by Meerwall *et al.* for the case $I = \frac{3}{2}$ where an analytical expression of the transition frequency derived from a first-order perturbation of degenerate levels has been used. Since the parameter $\nu_q = 40\nu_0$ is chosen in the exact calculation, a condition well suited for the first-order perturbation, identical results are expected.

The above critical frequencies (singularity, step, and the shoulder) are plotted versus the EFG asymmetry in Fig. 3. Note particularly the sensitivity to the EFG asymmetry of the resonance of the singularity frequency for the $I = \frac{7}{2}$ species. For example, a change in η from 0 to 0.3, shifts this singularity from $4\nu_0$ to $2\nu_0$. This is to be compared with the same change in η for spin $I = \frac{3}{2}$, where a shift of $0.3\nu_0$ is observed. Also notice the diminishing intensity of the singularity when η approaches 1 for spin $\frac{7}{2}$.

Experimentally, due to limited rf power and the width of this spectrum, signal intensity is barely observable other than at those critical frequencies mentioned above. Therefore, for either a transient or a cw NMR experiment, only the most prominent feature of the transition as mentioned above can be observed. These critical frequencies, particularly the singularity ($\mathbf{B}_0 \parallel \hat{\mathbf{X}}$), are much more intense than the rest of the powder pattern. Furthermore the width of the broadening function, Δ , in the calculation is much greater than one would expect experimentally. Therefore a more pronounced singularity intensity will be produced than those calculated. In the absence of a cw determination of the spectrum, or a spin-echo mapping, the use of single-shot transient determination of a complete powder line shape is not feasible. However information can still be extracted solely from a

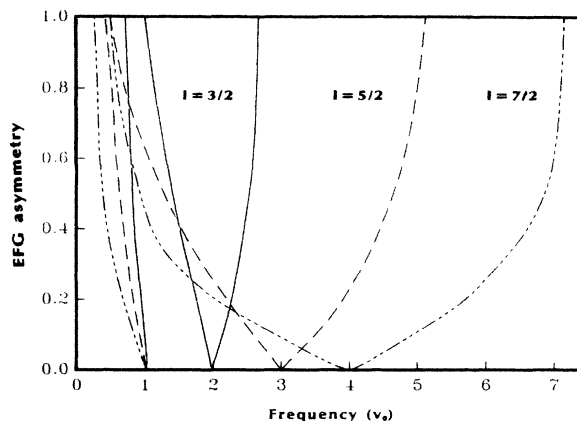


FIG. 3. The critical frequencies in the above calculation are drawn. The three critical frequencies correspond to three orientations of the EFG with respect to the magnetic field, denoted as $\parallel \hat{\mathbf{X}}$, $\parallel \hat{\mathbf{Y}}$, and $\parallel \hat{\mathbf{Z}}$. Due to the width of the spectra relative to the limited spectral width of the rf pulse only the critical frequencies can be observed in the pulse NMR experiment.

study of the critical frequencies. Hence a search of the resonance frequency is required as part of the experiment because the singularity will, in general, not occur near the Larmor frequency. For a strong quadrupolar spin $I = \frac{7}{2}$ species, this frequency may range from $0.3\nu_0$ to $4\nu_0$.

Unlike a pure NQR measurement, this NMR frequency is not sensitive to the quadrupole coupling constant. Even with a change of about 10% in the value of e^2qQ value, there is no observable change of the calculated results. Although the quadrupole coupling constant, in principle, also yields information concerning the change of the local electron structure at the lutetium site, this constant cannot be determined from the current variable temperature studies since the singularity frequency is almost independent of the quadrupole coupling constants. These constants, however, may be obtained through variable magnetic field studies similar to that proposed by Meerwal *et al.*¹⁵ and Segel *et al.*¹⁴

RESULTS AND DISCUSSION

All three compounds possess the same $\text{Sc}_5\text{Co}_4\text{Si}_{10}$ -type structure.¹⁷ In this structure the rare-earth metal may occupy at most three crystallographically distinguishable sites as shown in Fig. 1. As will be seen, the NMR resonances corresponding to these lutetium sites are well resolved.

Extensive studies of electronic phase transitions by NMR have been reported.^{7-13,23-26} In principal, modulation waves incommensurate with the periodicity of the crystal lattice can be categorized into two classes:²⁴ (1) In a metallic conductor, the conducting material, the structural phase transition is driven by strong electron-phonon coupling that favors a particular symmetry (or shape) of the Fermi surface. The periodicity of the charge-density wave determined by the Fermi surface may not be commensurate with the lattice periodicity. In order to minimize the Gibbs free energy of the sys-

tem, the lattice is periodically distorted, and the distortion is accompanied by the formation of a CDW. (2) In insulators, the incommensurate lattice modulation is a type of Jahn-Teller distortion which stabilizes the localized bonding. The phase transition between the normal metallic and the incommensurate PLD/ICDW states is accompanied by a weak anomaly in resistance and, in most of the systems studied, does not prevent the transition to a superconducting state at lower temperatures. Furthermore increasing pressure suppresses the formation of CDW's and induces the transition to the superconducting state.²⁷

Though the origins of the CDW state are different in metals and insulators, the influences on the NMR spectra are basically due to the periodic lattice distortion and, hence, can be described by the same line-shape theory. The influences of the formation of the PLD/ICDW state upon the NMR spectrum are qualitatively described as follows:^{11,24}

(1) A quasicontinuous distribution of the interaction parameters characterizing the EFG and the Knight shift interaction tensors is reflected in a sudden increase of the NMR line width upon the formation of the incommensurate state.

(2) A loss of the density of states at the Fermi level is reflected in a jump discontinuity of the isotropic Knight shift.

As mentioned previously, the NMR critical resonance frequency in the quadrupole regime is insensitive to the change of the quadrupole interaction. Use of the NMR line width characterized by the quasicontinuous distribution of either the quadrupole coupling constant or the shift anisotropy as a means to monitor the formation of the ICDW state is not feasible here. On the other hand, the singularity resonance frequencies correspond to $(1 - \sigma_{xx})\nu$, where ν is the singularity frequency calculated without considering the Knight shift anisotropy. This measurement clearly reflects the change of the electron density of states due to the relation of the Knight shift to the free electron density.

In the following, the NMR spectra of the three samples are discussed separately in terms of the temperature dependent Knight shifts.

NMR of $\text{Lu}_5\text{Ir}_4\text{Si}_{10}$

The variable temperature NMR spectra of lutetium at ambient pressure are shown in Fig. 4 for several chosen temperatures. In this experiment, the carrier frequency is located near the downfield resonance. Two groups of peaks can be observed at all temperatures. The intensity of the upfield peak which resonates about 600 kHz from the carrier frequency, is therefore severely attenuated.

From the calculation in the previous section, it is inferred that this spectrum characterizes the singularity of the powder spectra in the quadrupole regime. From Fig. 3, the singularity frequency is found to appear at $\nu \approx \nu_0$ when $\eta \approx 0.4$. In addition to a systematic upfield shift, the line shape of the spectrum changes gradually as the temperature increases. This upfield shift is found to be associated with the temperature dependence of the EFG

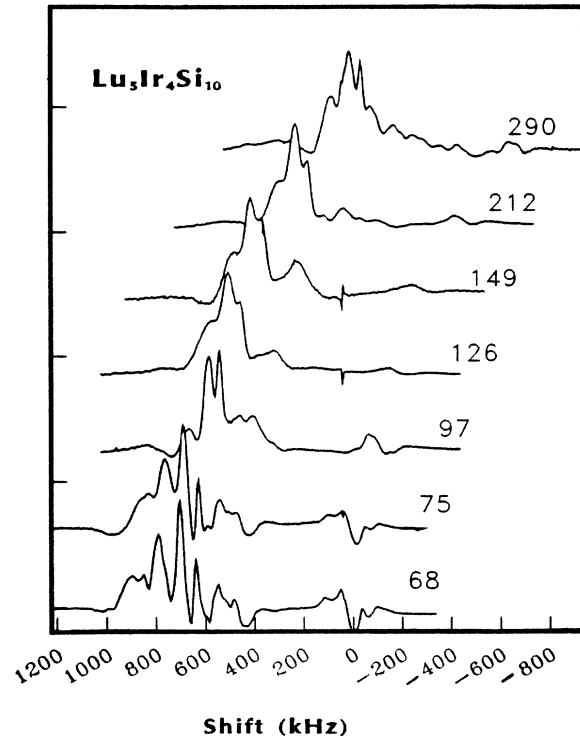


FIG. 4. Temperature dependence of the $(\frac{1}{2}, -\frac{1}{2})$ transition of ^{175}Lu in polycrystalline $\text{Lu}_5\text{Ir}_4\text{Si}_{10}$ sample at 25 MHz. The carrier frequency is set to be near the downfield resonance. Another peak resonating at ≈ 600 kHz upfield is severely attenuated.

asymmetry (*vide infra*). The line shape remains constant in the high-temperature region.

To correlate the shift with temperature, the position of the highest peak in the spectrum is plotted versus temperature in Fig. 5. Two kinks are observed in the temperature dependence of the peak position at 140 and 83 K. In the inset of Fig. 5, the expanded region of the electronic phase transition around 83 K is shown. The sudden drop of the shift as the temperature decreases is found to be associated with the loss of the density of states at the lutetium site (*vide infra*).

The upfield peak is not associated with the shoulder ($\mathbf{B}_0 \parallel \hat{\mathbf{Z}}$) of the spectra as that calculated in Fig. 2(c) and in Fig. 3. This conclusion follows from the observation that at $\eta = 0.4$, the spacing between the two critical frequencies ranges from $0.4\nu_0$ to $0.6\nu_0$, which equals about 10 to 15 MHz in the current magnetic field measured and is clearly too large to account for the 600 kHz difference. One probable origin for this peak may be associated with the lutetium nucleus of different sites which possess different EFG asymmetries and quadrupole coupling constants and shift anisotropies.

To better study the spectrum in the upfield region with the hope of obtaining different information about the electronic structure at different lutetium sites, the experiment was repeated for this compound with the carrier frequency located near the upfield resonance. The peak areas are about half of those obtained previously for the downfield peak at the corresponding temperature.

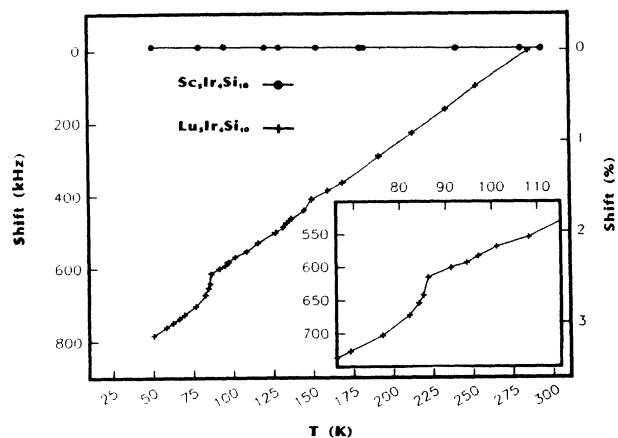


FIG. 5. Peak position vs temperature of lutetium NMR of $\text{Lu}_5\text{Ir}_4\text{Si}_{10}$ and ^{45}Sc in $\text{Sc}_5\text{Ir}_4\text{Si}_{10}$. Solid lines are drawn through the points to show the temperature variation of the shift. Kinks are observed at 83 and 140 K for the lutetium ternary compound. The inset shows the expanded region around 83 K.

Within this resonance, three well-resolved peaks are observed. The three peaks remain clearly separated until above the transition at 83 K, then the two upfield peaks gradually converge. Figure 6 shows the temperature variation of the frequency of these peaks. Three regimes can be observed in the behavior of this upfield transition:

(1) Above 90 K, a pretransitional broadening gradually takes place. Butaud *et al.* have demonstrated that impurities and crystal defects play important roles in such broadening in incommensurate-commensurate transitions.²⁸

(2) Below 79 K the singularity is resolved into two peaks. The splitting of those peaks gradually levels off at about 50 kHz upon further decrease in temperature. This behavior is observed in the single-crystal studies of several ICDW electronic phase transitions, where a

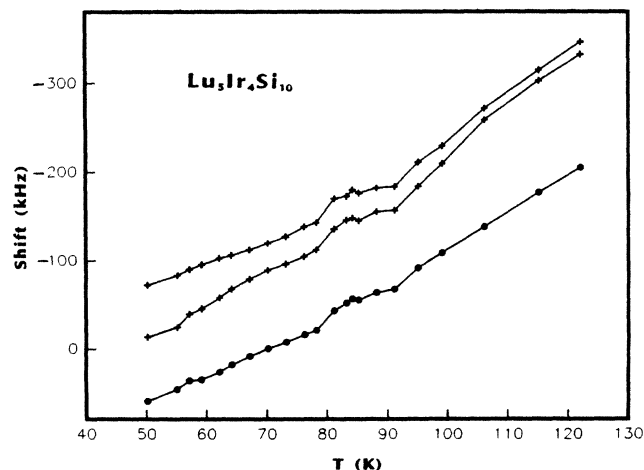


FIG. 6. The temperature dependence of the three peaks observed in the upfield resonance in $\text{Lu}_5\text{Ir}_4\text{Si}_{10}$. This experiment is performed exactly the same as the previous one, except that the carrier frequency is set to be near the upfield resonance. Both kinks and the change of slopes are observed above 83 K.

quasicontinuous distribution of the shift interaction parameters yield a two-peak feature separated by a few tens of kHz.

(3) Between 90 and 79 K, the individual resonance frequencies becomes less temperature dependent. This may represent the stage between the initiation and the finish of the phase transition.

The temperature coefficients of the shift frequency in the two regimes close to the transition are quite different. This difference gradually levels off to the average value. This behavior is also observed in the downfield resonance where the temperature coefficient close to the transition temperature is different, however the overall curve can be approximated by a linear relation with a slope of about 3 kHz/K.

When the sample is further cooled below 60 K the spectrum develops several sharp peaks with a total width of roughly 500 kHz. This feature may correspond to the formation of a discommensurate region where domain walls separating different commensurate waves are followed by a lock-in transition at the incommensurate-commensurate temperature (ICT). This phenomenon has been observed in several structural incommensurate and charge-density-wave incommensurate compounds when the system approaches the ICT temperature.^{10,11,28} However this behavior is not consistent in all ICDW transitions reported so far. The behavior in this temperature region requires further study.

NMR of $\text{Lu}_5\text{Rh}_4\text{Si}_{10}$

Similar to the results observed in $\text{Lu}_5\text{Ir}_4\text{Si}_{10}$, the NMR resonance of ^{175}Lu in $\text{Lu}_5\text{Rh}_4\text{Si}_{10}$ in the quadrupole regime shows two major resonances. These resonances correspond to the singularity ($\mathbf{B}_0 \parallel \hat{\mathbf{X}}$) associated with the perpendicular EFG orientation with the Zeeman field. The NMR spectra of the $(\frac{1}{2}, -\frac{1}{2})$ transition in the quadrupole regime of ^{175}Lu of this compound are shown in Fig. 7 as a function of the temperature.

To better observe the temperature dependence of the shift, the temperature variation of the resonance frequency of the highest peak of this transition is shown in Fig. 8. A kink at approximately 145 K is observed where it exhibits a frequency jump of approximately 25 kHz. This kink is smaller than the jump of about 50 kHz found in the $\text{Lu}_5\text{Ir}_4\text{Si}_{10}$ at 83 K. The difference in these changes in the two samples is consistent with the behavior of the magnetic susceptibilities of the two compounds (*vide infra*). Another kink at 90 K seems to be reproducible. However, it is barely discernible from the noise and will not be further mentioned.

Below 60 K the spectrum changes in a manner similar to that observed for $\text{Lu}_5\text{Ir}_4\text{Si}_{10}$. The transition gradually broadens and splits into several relatively sharp lines with a total width of approximately 500 kHz.

In summary, results of NMR, resistivity and susceptibility measurements indicate that the electronic transitions in $\text{Lu}_5\text{Ir}_4\text{Si}_{10}$ and $\text{Lu}_5\text{Rh}_4\text{Si}_{10}$ have the characteristics of the formation of an incommensurate-charge-density wave. A search for direct evidence of a periodic lattice distortion accompanied with the formation of an

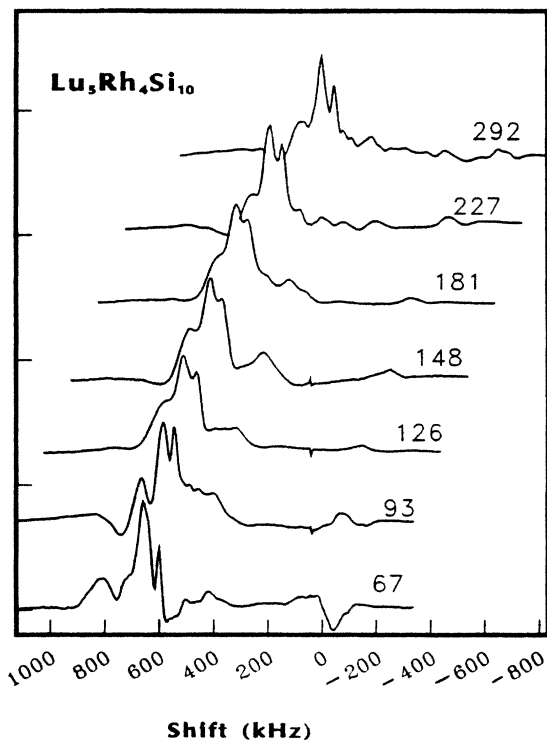


FIG. 7. Temperature dependence of the ($\frac{1}{2}$, $-\frac{1}{2}$) transition of ^{175}Lu in polycrystalline $\text{Lu}_5\text{Rh}_4\text{Si}_{10}$ sample at 25 MHz. The intensity of the upfield resonance is reduced due to the peak being ≈ 600 kHz off resonance from the carrier frequency.

ICDW state in these two compounds by low-temperature single-crystal x-ray diffraction is underway. It would be of interest to see if a band structure calculation for these materials would yield the possibility of forming a charge-density-wave state in these compounds.

NMR of $\text{Sc}_5\text{Ir}_4\text{Si}_{10}$

As a baseline measurement for comparison with the behavior of $\text{Lu}_5\text{Ir}_4\text{Si}_{10}$ and $\text{Lu}_5\text{Rh}_4\text{Si}_{10}$, the NMR of ^{45}Sc

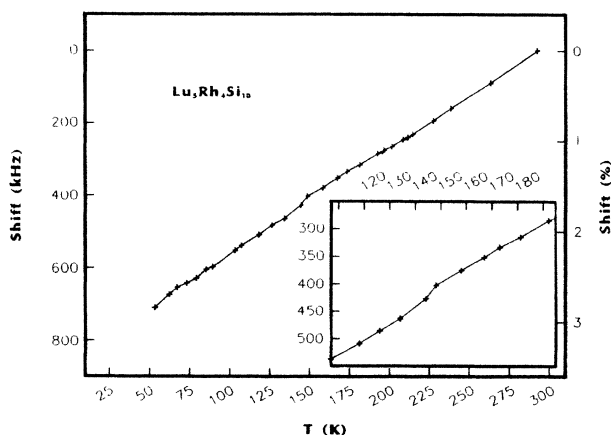


FIG. 8. Peak position of $\text{Lu}_5\text{Rh}_4\text{Si}_{10}$ vs temperature. A solid line is drawn through the points to show the variation of the curve in these regions. A kink at 145 K is seen, while the small variation around 90 K is approximately the same as the scatter in the data. The expanded region around 145 K is shown in the inset.

($I = \frac{7}{2}$) in $\text{Sc}_5\text{Ir}_4\text{Si}_{10}$ was determined as function of temperature. This compound exhibits no anomalies in resistivity or magnetic susceptibility in the temperature range of 2.4–300 K. The temperature variation of the center of mass of ^{45}Sc ($I = \frac{7}{2}$) NMR is smooth and changes monotonically with temperature. The isotropic value shifted downfield of 8 kHz from 79 to 293 K and no kink within experimental error can be detected, reflecting the expected behavior of a normal conductor. The shift versus temperature is shown in Fig. 5 for comparison with results of the downfield resonance of $\text{Lu}_5\text{Ir}_4\text{Si}_{10}$.

EFG asymmetry and the shift

In the high temperature, commensurate region of the compounds $\text{Lu}_5\text{Ir}_4\text{Si}_{10}$ and $\text{Lu}_5\text{Rh}_4\text{Si}_{10}$, the Knight shift for lutetium is expected to be independent of temperature and should behave like those of a normal metal. Experimentally this has not been observed, instead, the shift is strongly temperature dependent with a temperature coefficient of approximately 3 kHz/K as seen from Figs. 5 and 8. Although the shift clearly shows a kink at the transition temperatures, indicative of a loss of density of states at Fermi level, the large temperature-dependent upfield shift of approximately 3 kHz/K (120 ppm/K) of the two lutetium compounds is unexpected if the change of resonance frequency is governed by the Knight shift. This shift is not related to Curie-Weiss paramagnetism where one expects Knight shift to show an inverse temperature relation which is contradictory to the current observation.

There are at least two other causes of temperature (or pressure) dependence of the NMR resonance frequency in the quadrupole regime; these are the external thermal and mechanical influences on both the coupling constant and the asymmetry parameter. Therefore it is reasonable to attribute the highly temperature-dependent shift to the temperature-dependent EFG asymmetry as concluded from the previous calculation. For a spin $I = \frac{7}{2}$ species, the coefficient $\partial\eta/\partial\nu$, is estimated to be $\approx 10^{-5}/\text{kHz}$ from the calculation in the vicinity of ν_0 which equals roughly the carrier frequency in the current measurement. The 3 kHz/K upfield shift observed therefore corresponds to $\partial\eta/\partial T \approx 3 \times 10^{-5}/\text{K}$ increase of the EFG asymmetry. This asymmetry temperature coefficient is typical of the quadrupole nucleus where positive values of 10^{-4} to $10^{-5}/\text{K}$ has been reported from NQR measurement.²⁹

This temperature dependence of the asymmetry parameter is closely related to the temperature dependence of the volume of the sample and the coefficient $\partial\eta/\partial T$ is directly related to the thermal expansion coefficient and the bulk modulus of the sample. From the absence of the sudden change with temperature of these two quantities from the previous measurement,² the observed constant behavior of the asymmetry temperature coefficient is therefore also expected. The implication of such a small and constant change of the asymmetry indicates an absence of the change of the cohesive energy and of the change of the crystal structure in the samples. Hence it

is concluded that the observed electronic phase transition is not related to a first-order phase transition.

The recognition that the large upfield shift of the singularity frequency is due to the change of the EFG asymmetry allows us to isolate contributions of the Knight shift from the conduction electrons as will be discussed in the following.

Knight shift versus magnetic susceptibility

For a normal metal, the Knight shift is related to the density of electrons at the nucleus $P_f = |\langle U_k(0) \rangle^2|_{ef}$ and the magnetic susceptibility χ as indicated by Eq. (1),

$$K_{\text{iso}} = \frac{8\pi}{3} P_f \chi_e. \quad (1)$$

The Knight shift is very weakly temperature dependent since the wave-function density P_f at the nucleus and the electronic susceptibility χ_e are both independent of the temperature in general.³⁰

The temperature dependence of the Knight shift in the region of the incommensurate structural transition can be attributed to either the temperature dependence of the modulation vector or the density of electronic wave functions, or the temperature dependence of the magnetic susceptibility.

To relate the magnetic susceptibility to the Knight shift, one may start with the relations:

$$\begin{aligned} \chi_0 &= \chi^{\text{core}} + \chi^{\text{Pauli}} + \chi^{\text{Landau}} \\ &= \chi_{\text{dia}} + \chi_p^s + \chi_p^d + \chi_{vv}, \end{aligned} \quad (2)$$

where $\chi^{\text{core}} = \chi_{\text{dia}}$ is the diamagnetic susceptibility of the ion core; $\chi^{\text{Pauli}} = \chi_p^s + \chi_p^d$ is the Pauli paramagnetism, where two distinct contributions can be found, one from the conduction electron spins (d or f) and one from the itinerant s electrons. $\chi^{\text{Landau}} = \chi_{vv}$ is the diamagnetic orbital contribution due to the conduction electrons. The only term in the above equation expected to be sensitive to temperature is the spin susceptibility χ^{Pauli} . To a first approximation, this term is found to be linearly proportional to the density of states $\rho_s(E_F)$ of the s and to $\rho_d(E_F)$ of the d electrons individually at the Fermi level. The value of $\rho_d(E_F)$ is usually 10 to 20 times larger than $\rho_s(E_F)$ therefore d or f electrons are expected to play a crucial role in this change.

Similar to the individual contributions to the magnetic susceptibility there are assumed to be three distinct contributions to the Knight shift: (1) an S contact part which results from the paramagnetism of the S -band electrons at the Fermi surface, (2) a core polarization contribution which results indirectly from the spin paramagnetism of the d electrons, and (3) an orbital contribution from the conduction electrons. The core diamagnetic contribution to the chemical shift can be completely neglected due to its small magnitude relative to the other terms. In summary, the contributions to the Knight shift in a transition metal can be expressed as³¹

$$\begin{aligned} K(T) &= K_s + K_d(T) + K_{vv} \\ &= 0.895 \times 10^{-4} H_s \chi_p^s - 0.895 \times 10^{-4} H_d \chi_p^d(T) \\ &\quad + 22.6 \langle r^{-3} \rangle \chi_{vv}. \end{aligned} \quad (3)$$

H_s and H_d are the electronic spin hyperfine magnetic fields at the nucleus and measured in Oe, and all the magnetic susceptibilities are in units of emu/mol. Using temperature as an implicit variable and assuming that χ_p^d is the dominate term in (3), the behavior of $K(\chi_0)$ is linear with a negative slope of $-0.895 \times 10^{-4} H_d$. From the correlation of the temperature dependent Knight shift and the magnetic susceptibility the hyperfine field H_d can be obtained. The fact that in a number of transition metal compounds, a plot of $K(T)$ versus $\chi(T)$ is a straight line with positive slope,³² supports the model proposed here.^{6,26,31,33} In Fig. 9, the total shift is plotted against the susceptibility at the same temperature. The linear behavior of $\text{Lu}_5\text{M}_4\text{Si}_{10}$ ($M = \text{Ir}, \text{Rh}$) inferred from the above discussion is however not observed. The discrepancies can also be inferred in the high-temperature measurements region where $\chi(T)$ is temperature independent,² while $K(T)$ is still linearly dependent upon the temperature.

As concluded from the previous section that the total shift observed is contributed both from the temperature dependence of the EFG asymmetry as well as the Knight shift. Assuming that within 1 MHz of the vicinity of the experimental frequency $\nu_0 = 25$ MHz, $\nu(\eta)$ is linear (Fig. 2), the temperature coefficient of the asymmetry, $\partial\eta/\partial T$ can be considered to be constant $= 3 \times 10^{-5}/\text{K}$. As observed from Figs. 5 and 8, the "background" upfield shift due to a small change in asymmetry is also close to being linear. To obtain the Knight shift contribution, the 3 kHz/K linear "background" due to the EFG asymmetry change is subtracted from the total shift. The Knight shift versus conduction electron susceptibility is now linear as shown in the fitted solid lines superimposed with the total shift data of the corresponding curves in Fig. 9.

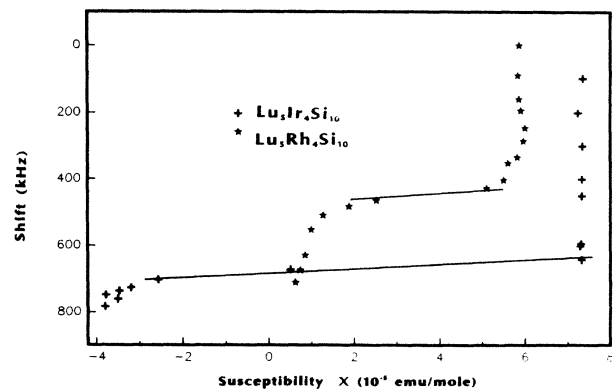


FIG. 9. $K_{xx}(\chi_0)$ for both $\text{Lu}_5\text{Ir}_4\text{Si}_{10}$ and $\text{Lu}_5\text{Rh}_4\text{Si}_{10}$, with temperature an implicit variable. The solid curves represent the Knight shift contribution vs χ_0 after subtraction of the 3 kHz/K background shift due to the temperature-dependent EFG asymmetry. From the slope, the hyperfine fields are calculated to be 0.5 and 0.7 MOe, respectively, for $\text{Lu}_5\text{Ir}_4\text{Si}_{10}$ and $\text{Lu}_5\text{Rh}_4\text{Si}_{10}$.

Note that the two lutetium compounds show a similar slope implying that the hyperfine field for the lutetium sites are quite similar. This result together with the jump in magnetic susceptibility by a factor of two at the transition temperature also accounts for the similar ratio of jump in the Knight shift for the two compounds. From the slope of $K(\chi)$ curve, the hyperfine field is calculated to be 0.5 and 0.7 MOe, respectively, for $\text{Lu}_5\text{Ir}_4\text{Si}_{10}$ and $\text{Lu}_5\text{Rh}_4\text{Si}_{10}$. These fields correspond to hyperfine frequencies of 230 and 330 MHz, respectively, and are consistent with the decreasing trend of the hyperfine frequency from ^{165}Ho (6467 MHz) to ^{167}Er (913 MHz) rare-earth metal measured by NQR.⁶ These values are in good agreement with another hyperfine field measurement from perturbed angular distribution of diluted Lu in Fe host which is found to be 0.483 MOe.³⁴

Another source of the temperature-dependent "background" shift may be associated with the s -electron contact interaction, which produces a linear change of K_s versus temperature. As mentioned previously, χ_p^s is much less temperature dependent than χ_p^d due to the fact that the density of S states at the Fermi surface, $\rho_s(E_F)$ is one or two orders less than $\rho_d(E_F)$. Hence, the contribution of χ_p^s is almost temperature independent. To override the contribution from $K_d(T)$ and yield such a large linear background shift, the contact hyperfine field, H_s , must be extremely large. This field, proportional to the s electron density at nucleus does not seem too likely to account for such a temperature sensitive shift and is dismissed as the source of the background.

CONCLUSION

Changes in the electronic environment of the quadrupolar nucleus lutetium below 83 K in $\text{Lu}_5\text{Ir}_4\text{Si}_{10}$ and below 145 K for $\text{Lu}_5\text{Rh}_4\text{Si}_{10}$ have been inferred from the NMR of ^{175}Lu ($I = \frac{7}{2}$) in the quadrupole regime for bulk samples. This experiment uses the fact that the singularity is the most prominent feature which can be observed in the pulse NMR experiment of a nucleus with a large quadrupole moment. This frequency, corresponding to the x axis of EFG tensor being parallel to the magnetic field, is quite sensitive to both the change of the EFG asymmetry and the Knight shift. Therefore, this feature becomes a valuable tool in the detection of electronic phase transitions observed in these compounds.

The singularity for ^{175}Lu NMR appeared at $\nu \cong \nu_0$ for both compounds, indicating that the EFG asymmetry for lutetium is close to $\eta \cong 0.4$. The temperature-dependent resonance curve shows jump discontinuities at the transition temperature, reflecting a loss of density of electronic states at the Fermi level due to the opening of

the energy gap by a Peierls-type phase transition. This behavior is consistent with the notion of the formation of an incommensurate-charge-density-wave state. The strong temperature dependence of the "background" lutetium Knight shift, about 3 kHz/K (120 ppm/K) is found to be related to the temperature variation dependence of the EFG asymmetry parameter. From this the temperature coefficient, $\partial\eta/\partial T$ is calculated to be $3 \times 10^{-5}/\text{K}$. The presence of a first-order phase transition has been excluded since: (1) there is a very small change in asymmetry of the EFG, and (2) x-ray-diffraction data for powder samples do not exhibit extra diffraction lines around this temperature.

After the temperature-dependent shift due to the change of the EFG asymmetry has been subtracted from the total shift of NMR measurements, the Knight shift contribution is found to correlate well with the anomalous behavior of the resistivities and the magnetic susceptibilities of these samples (reference). The ratio of the amplitude of jump in the NMR frequency for $\text{Lu}_5\text{Ir}_4\text{Si}_{10}$ at 83 K and $\text{Lu}_5\text{Rh}_4\text{Si}_{10}$ at 145 K is consistent with the ratio of the amplitude of anomalies in both the resistivities and magnetic susceptibilities. The similar slopes shown in the $K(\chi)$ plot (Fig. 9) imply that the hyperfine coupling constants are roughly the same in both compounds, estimated to be 0.5 MOe for $M = \text{Ir}$ and 0.7 MOe for $M = \text{Rh}$ from the slope. This hyperfine field is reasonable in comparison with other rare-earth metals.

Another transition not observed in the resistivity and the magnetic susceptibility was observed in NMR at 140 K for $\text{Lu}_5\text{Ir}_4\text{Si}_{10}$ which may be associated with the presence of an incommensurate structural phase. This modulation wave possesses a relatively small amplitude when compared with the periodic lattice distortion of the ICDW state as inferred from the smaller frequency jump at 140 K in the Knight shift variation.

^{45}Sc NMR of $\text{Sc}_5\text{Ir}_4\text{Si}_{10}$, a material with no anomalous behavior in the resistivity or susceptibility has also been measured from 79 to 293 K. The variations of the center of mass, and of the quadrupole constants are smooth and monotonic, and give no indication of a phase transition from the NMR measurement.

ACKNOWLEDGMENTS

Helpful discussions with Dr. R. G. Barnes about relations between magnetic susceptibility and the Knight shift are greatly acknowledged. Also thanks to Dr. Russel Walker who helped with the low-temperature measurements. This research was supported by the U.S. Department of Energy (Basic Energy Sciences Program, Chemical Science Division), under Contract No. W-7405-Eng-82.

¹R. N. Shelton, L. S. Hausermann-Berg, P. Klavins, H. D. Yang, M. S. Anderson, and C. A. Swenson, *Phys. Rev. B* **34**, 4590 (1986).

²H. D. Yang, R. N. Shelton, and H. F. Braun, *Phys. Rev. B* **33**,

5062 (1986).

³C. Kittel, *Introduction to Solid State Physics* (Wiley, New York, 1986), p. 285.

⁴B. C. Gerstein and C. R. Dybowski, *Transient Techniques in*

- NMR: An Introduction to the Theory and Practice* (Academic, New York, 1985).
- ⁵R. G. Barnes, in *Handbook on the Physics and Chemistry of Rare Earths*, edited by K. A. Gschneider, Jr. and L. Eying (North-Holland, Amsterdam, 1979), Vol. 2, p. 387.
- ⁶M. A. H. McCausland and I. S. Mackenzie, *Adv. Phys.* **28**, 305 (1979).
- ⁷N. P. Ong, *Phys. Rev. B* **17**, 3243 (1978).
- ⁸N. P. Ong and P. Monceau, *Phys. Rev. B* **16**, 3443 (1977).
- ⁹C. Berthier, D. Jerome, and P. Molinie, *Solid State Phys.* **11**, 797 (1978).
- ¹⁰J. H. Ross, Jr., Z. Wang, and C. P. Slichter, *Phys. Rev. Lett.* **56**, 663 (1986).
- ¹¹*Incommensurate Phases in Dielectrics, Fundamentals* Vol. 14.1, in *Modern Problems in Condensed Matter Sciences*, edited by R. Blinc and A. P. Levanyuk (North-Holland, Amsterdam, 1986), and the references therein.
- ¹²F. Devreux, *J. Phys. (Paris)* **43**, 1489 (1982).
- ¹³M. Natio, H. Nishihara, and S. Tanaka, *Solid State Phys. C* **16**, L387 (1983).
- ¹⁴S. L. Segel and R. G. Barnes, *Phys. Rev. Lett.* **15**, 886 (1965).
- ¹⁵E. D. von Meerall, R. B. Creel, C. F. Griffin, and S. L. Segel, *J. Chem. Phys.* **59**, 5350 (1973).
- ¹⁶D. L. Macalady and R. G. Barnes, *Chem. Phys. Lett.* **5**, 186 (1970).
- ¹⁷H. F. Braun, K. Yvon, and R. M. Braun, *Acta Crystallogr. B* **36**, 2397 (1980).
- ¹⁸T. T. P. Cheung, L. E. Worthington, P. D. Murphy, and B. C. Gerstein, *J. Magn. Reson.* **41**, 158 (1980).
- ¹⁹D. Freude, J. Hass, J. Kleinowski, T. A. Carpenter, and G. Ronikier, *Chem. Phys. Lett.* **119**, 365 (1985).
- ²⁰D. J. Adduci, P. A. Hornung, and D. R. Torgeson, *Rev. Sci. Instrum.* **47**, 1503 (1976).
- ²¹T. P. Das and E. L. Hahn, *Solid State Phys. Suppl.* **1**, 12 (1958); M. Toyama, *J. Phys. Soc. Jpn.* **14**, 1727 (1959); A. T. Nicol, Ph.D. thesis, California Institute of Technology, 1980.
- ²²P. J. Chu, Ames Laboratory report, 1987 (unpublished). This calculation uses an IMSL Library routine to perform the matrix diagonalization in determining the eigenvalues and the eigenvectors in the presence of both quadrupolar and Zeeman interactions. The eigenvector is later used to determine the transition probability which is required in the calculation of the spectrum.
- ²³R. Blinc, V. Rutar, and F. Milia, *Phys. Rev.* **23**, 4577 (1981).
- ²⁴R. Blinc, V. Rutar, J. Seliger, S. Zumer, T. Rasing, I. P. Aleksandrova, and F. Milia, (unpublished).
- ²⁵R. Blinc, V. Rutar, B. Topic, F. Milia, and P. Aleksandrova, *Phys. Rev. Lett.* **46**, 1406 (1981).
- ²⁶A. V. Skripov, A. P. Stepanov, A. D. Shevchenko, and Z. D. Kovalyuk, *Phys. Status Solidi* **119**, 401 (1983).
- ²⁷F. J. Disalvo, in *Electron-Phonon Interactions and Phase Transitions*, edited by T. Riste (Plenum, New York, 1979), p. 107.
- ²⁸P. Butaud, P. Segransan, C. Berthier, J. Dumas, and C. Schlenker, *Phys. Rev. Lett.* **55**, 253 (1985).
- ²⁹N. E. Ainbinder and I. G. Shaposhnikov, in *Advances in Nuclear Quadrupole Resonance*, edited by J. A. S. Smith (Heyden & Son Ltd., London, 1978), Vol. 3, p. 67.
- ³⁰C. P. Slichter, *Principles of Magnetic Resonance*, Vol. 1 of *Springer Series in Solid State Sciences*, 2nd ed., edited by M. Cardona, P. Fulde, and H. J. Queisser (Springer-Verlag, Berlin, 1978).
- ³¹A. J. Freeman and R. E. Watson, in *Magnetism*, edited by G. T. Rado and H. Suhl (Academic, New York, 1973).
- ³²The current study uses the δ scale for the Knight shift. If the σ scale were used, i.e., larger shift values corresponding to lower field, then the slope of $K(\chi)$ plot would be negative.
- ³³V. Jaccarino, in *Proceedings of the International School, Course XXXVII*, edited by W. Marshall (Academic, New York, 1967), p. 335.
- ³⁴T. A. Koster and D. A. Shirley, in *Hyperfine Interactions in Excited Nuclei*, edited by G. Goldring and R. Kalish (Gorden and Breach Science, Paris, 1971), p. 1244.